Posture-Specific Spatial Calibration for Kinematic Model Optimization based on Human Activity Recognition in Ergonomic Evaluations

Sergio Leggieri[1], Darwin Caldwell[1] and Christian Di Natali[1]

***Abstract*— Work-related musculoskeletal disorders (WMSDs) constitute the most prevalent occupational injury in manual material handling (MMH) across Europe. WMSDs lead to significant socio-economic losses. Multiple observational methods have related working conditions and ergonomics in MMH and workplaces to the risk of developing WMSDs for targeted and informed risk mitigation strategies. Digital ergonomic evaluations represent the next step in this process, complementing observational methods with statistical analysis and monitoring the evolution of risks over time. IMU-based motion capture technologies play a key role in this perspective due to their ease of integration into worker suits. However, IMU sensors are prone to estimation errors that affect the user kinematic and the task reconstruction. Optimization techniques, human activity recognition algorithm, and the posture-specific spatial calibration (PSSC) can refine the accuracy of whole-body kinematic models, enabling precise ergonomic assessments in real-time. This pilot study analyzes a standard MMH activity. Applying the proposed PSSC, the user kinematics is reconstructed with an average error of 50 mm. The optimized model improves the ergonomic risk evaluation by 60% w.r.t. the non-optimized one. Compared to the observational method, the lifting index of the digital ergonomic evaluation differs by 0.05, representing the 1.6% of the full-scale.**

I. INTRODUCTION

The most widespread health issues that affect workers across Europe are the work-related musculoskeletal disorders (WMSDs), accounting for 60% of the total, as reported by the European Agency for Safety and Health at Work survey [1]. WMSDs account for 40% of the cost of worker compensation, leading to a reduction of 1-2% in the gross domestic product of individual member states. Therefore, promoting good practices that aim to prevent and/or reduce the incidence of WMSDs would improve worker well-being, generating positive effects on companies and society.

Currently, manual material handling (MMH) activities and associated work tasks regulated by ISO 11228-1 are scrutinized by ergonomists during field inspections that aim to evaluate the quality of working environments and actions performed by workers. Through observational methods such as the NIOSH lifting equations [2], ergonomic risk indices are calculated according to tasks, type of activities, and body segments involved. However, observational methods are prone to errors, simplifications, and details may go unnoticed [3]. Instead, digital ergonomic evaluations provide standardized procedures, complementing the assessment with statistical analysis that can report any evolution of the risk over time. Motion capture (MoCap) technologies play a key role in this context, enabling constant tracking of workers during shifts [4].

State-of-the-art MoCap solutions include optical and wearable systems. Vision-based solutions offer a tracking accuracy of 2.0 mm and are considered the gold standard in the research field. However, they are limited in range and require calibrated cameras with a clear line of sight, making them impractical in industrial settings [5]. MEMS-based wearable technologies are emerging as an alternative to camera-based systems for real-world, large-scale, industrial assets. Due to the nature of sensing elements, most of the IMU-based suits are affected by electromagnetic interference (EMI), leading to poor tracking performance over time. Moreover, commercial IMU-based systems can produce angular errors ranging from 3 to 6 degrees, generating large Cartesian errors (approximately 10% of link length) in whole-body kinematic models of workers. Nonetheless, IMU-based suits have been used to assess ergonomic risks in MMH activities [4] and to identify complex activities carried out in occupational scenarios through Human Activity Recognition (HAR) algorithms [6]. To tackle the EMI sensitivity, industrial wearable systems (IWS) have been developed with magnetometer-free IMUs that provide reliable results even in electromagnetic environments [7]. Additionally, optimization methods have been proven effective in improving the real-time tracking accuracy in IMU-based systems, reducing the pose estimation errors to 50 mm in whole-body kinematic models [8]

In this work, we use an IMU-based IWS to track the user motion during a common MMH activity and to evaluate online the task-related ergonomic risk according to the NIOSH lifting index. Performing a posture-specific spatial calibration (PSSC), we generate 3D maps of optimal parameters by solving a nonlinear optimization problem. During the activity, a rule-based HAR algorithm identifies the user posture and the corresponding map. This allows to select online the parameters that optimize the whole-body kinematic model, increasing the accuracy of the user pose estimation. Finally, we identify all the phases of the MMH activity and evaluate, online, the corresponding NIOSH lifting index.

II. MATERIALS AND METHODS

The Total-Body Smart Suit (TB-SS) is an IWS that integrates IMUs and surface electromyography sensors (sEMG) into a high-visibility work clothing often used by workers

This work was supported by the BEEYONDERS project funded by the European Union's Horizon Europe research and innovation programme under grant agreement N° 101058548.

[1] is with Department of Advanced Robotics, Istituto Italiano di Tecnologia, 16163 Genova, Italy;
corresponding: sergio.leggieri@iit.it;
darwin.caldwell@iit.it;
christian.dinatali@iit.it

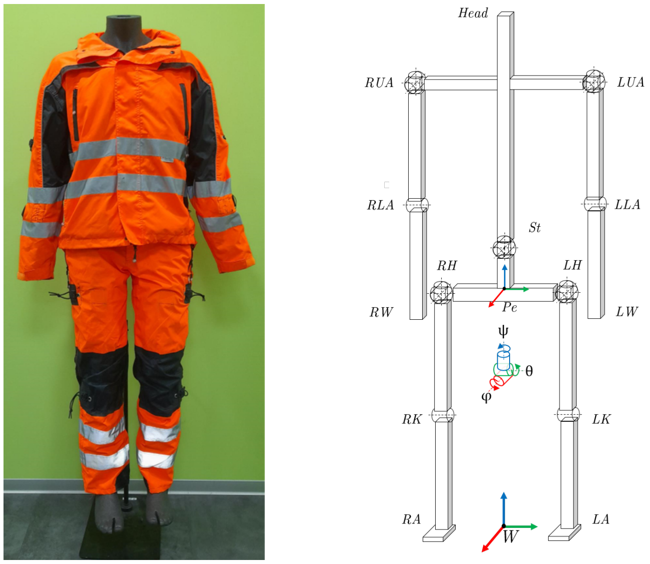

(a) (b)

Fig. 1. (a) The Total-Body Smart Suit design and the general overview [7]. Ten magnetometer-free IMUs are distributed symmetrically in the high-visibility work clothing. In each sleeve, the TB-SS integrates an EMG-based armband. (b) Schematic representation of the kinematic model and illustration of the "virtual" joint that relates the pelvis Pe frame with the inertial frame W [8].

[7]. It has been designed to monitor worker movements and interactions with the environment, allowing to be worn easily without supervision. Referring to Figure 1a, ten magnetometer-free IMUs are placed symmetrically on the user in the shanks, thighs, pelvis, sternum, upper and lower arms. The two EMG sensors, with eight electrodes each, are in direct contact with the skin of the forearms.

A. Kinematic Model

The TB-SS IMU sensors collect inertial data that are used to calculate the user kinematics, i.e., the Cartesian position of each body segment. This serial kinematic model has twelve links connected by nine joints for a total of twenty-two Degrees of Freedom (DoFs). Once the orientation of the inertial frame W is established, as in Figure 1b, local frames are defined on each joint and link of the model. The frame Pe that is placed in the middle of the pelvis acts as the root of the entire model. Referring to Figure 1b, a 3 degrees of freedom (DoFs) "virtual" joint relates the orientation of the frame Pe w.r.t. the inertial frame W as consecutive Roll-Pitch-Yaw (RPY) rotations. The right and left hips (RH, LH) are represented as spherical joints with 3 DoFs. The knees (RK, LK) are modeled as revolute joints with a 1 DoF. The ankle joints (RA, LA) are not modeled and the feet are fixed to the lower legs. The spine is modeled as a rigid link connected to the pelvis by a spherical joint (St). The clavicle-scapula complex is not modeled, and the shoulders are fixed on the sternum. The upper arms are connected to the shoulders with two spherical joints (RUA, LUA, and the elbows are represented as revolute joints (RLA, LLA) with one DoF each. The wrists are assumed to be rigidly attached to the forearms. The following homogeneous matrix describes the orientation of the frame Pe w.r.t. the inertial frame W:

$$T_{Pe}^{W}(\mathbf{\Phi}) = \begin{bmatrix} c_\psi c_\theta & -c_\theta s_\psi & s_\theta & 0 \\ c_\phi s_\psi + c_\psi s_\phi s_\theta & c_\phi c_\psi - s_\phi s_\psi s_\theta & -c_\theta s_\phi & 0 \\ s_\phi s_\psi - c_\phi c_\psi s_\theta & c_\psi s_\phi + c_\phi s_\psi s_\theta & c_\phi c_\theta & 0 \\ 0 & 0 & 0 & 1 \end{bmatrix} \quad (1)$$

where, $c(\cdot)$ and $s(\cdot)$ represent the cosine and sine functions, respectively. The angles $\mathbf{\Phi} = [\phi \;\; \theta \;\; \psi]^T$ are the RPY angles measured by the IMU sensor placed on the TB-SS belt. The joint vector $\mathbf{q}(t) \in \mathbb{R}^{22}$ collects the angles $\mathbf{\Phi}$, and all the relative joint angles $q_i(t)$ of each i-th DoF of the model. The whole-body kinematics is defined using the D-H parameters, starting from the pelvis frame Pe. where, the joint variable q_i corresponds to θ_i or d_i if the joint is revolute or prismatic, respectively. The position and orientation of each local frame w.r.t. the pelvis frame can be calculated as follows:

$$T_n^{Pe}(\mathbf{q}) = \Pi_{i=1}^{n} A_i^{i-1}(q_i) \quad (2)$$

where, $A_i^{i-1}(q_i)$ represents the homogeneous matrix of frame i w.r.t. frame $i-1$. The variable n represents the last link in the kinematic chain. To reconstruct the real location of the pelvis, our algorithm updates the pelvis position according to the current midpoint among the feet

$$\mathbf{p}_{Pe}^{W}(t) = \mathbf{p}_{Pe}^{'}(t) - \overline{\mathbf{p}}_A(t) \quad (3)$$

where, $\overline{\mathbf{p}}_A(t)$ represents the midpoint among the feet. This quantity is subtracted also from all the model segments.

B. Posture Specific Spatial Calibration

The objective of the posture-specific spatial calibration (PSSC) is to have the user kinematic model converge to the true 3D space position, compensating for the errors in IMU angular estimations. The parameter vector $\mathbf{a} = \left[\boldsymbol{\alpha}_1^T; \boldsymbol{\alpha}_2^T\right]^T \in \mathbb{R}^{44}$ combines scaling factors $\boldsymbol{\alpha}_1 \in \mathbb{R}^{22}$ and angular offsets $\boldsymbol{\alpha}_2 \in \mathbb{R}^{22}$ that parameterize the vector of joint angles $\mathbf{q}(t)$ as follows

$$\mathbf{q}(\mathbf{a}, t) = \boldsymbol{\alpha}_1 \circ \mathbf{q}(t) + \boldsymbol{\alpha}_2 \quad (4)$$

where the symbol $\circ$ represents the Hadamard product, i.e., the element-wise multiplication. Starting from a set of parameters $\mathbf{a}_0 = \left[\mathbf{1} \in \mathbb{R}^{22};\ \mathbf{0} \in \mathbb{R}^{22}\right]^T$, the midpoint among the hands is calculated as

$$\overline{\mathbf{p}}_W(\mathbf{a}, t) = \frac{\mathbf{p}_{RW}(\mathbf{a}, t) + \mathbf{p}_{LW}(\mathbf{a}, t)}{2} \quad (5)$$

where $\mathbf{p}_{RW}$ and $\mathbf{p}_{LW}$ are the positions of the right and left wrist, respectively. Over P_k desired points at the workspace boundaries, the spatial calibration is performed by solving the following nonlinear optimization problem

$$\begin{aligned} \min_{\mathbf{a}(k)} \quad & f(\mathbf{a}(k)) \\ \text{s.t.} \quad & \mathbf{lb} \leq \mathbf{a}(k) \leq \mathbf{lb} \end{aligned} \quad (6)$$

where, $\mathbf{a}(k)$ corresponds to the vector of optimal parameters for the point P_k, $\mathbf{lb}$ and $\mathbf{ub}$ represent the lower and upper

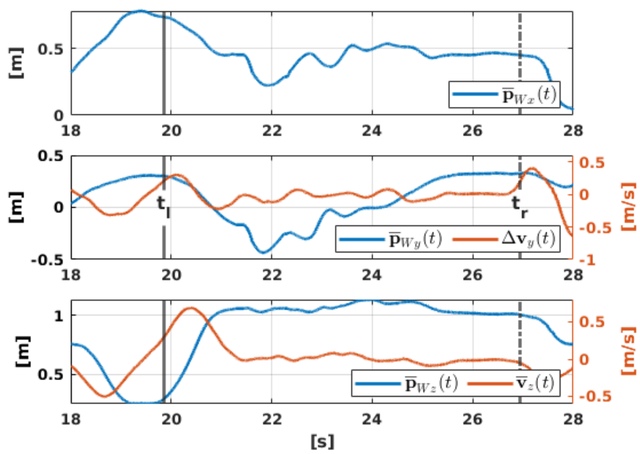

Fig. 2. Event detection algorithm (EDA) estimation of time of lift t_l and time of release t_r. From top to bottom, the x, y, and z components of the midpoint between the hands $\overline{\mathbf{p}}_W(t)$, the relative velocity $\Delta\mathbf{v}_{Wy}(t)$, and the average velocity $\overline{\mathbf{v}}_{Wz}(t)$.

bounds of $\mathbf{a}(k)$. The cost function $f(\mathbf{a}(k))$ has been defined as

$$f(\mathbf{a}(k)) = \mathbf{e}^T\mathbf{e} \tag{7}$$

with $\mathbf{e}(\mathbf{a}, k) = \overline{\mathbf{p}}_W(\mathbf{a}, k) - P_k$, which represents the error w.r.t. the known point P_k. The optimization is repeated for all the P_k desired points and produces a set of k vectors $\mathbf{a}(k)$, which are scattered at the edges of the workspace. To generate smooth surfaces of parameters, we define the Cartesian surfaces S_{z_1} and S_{z_2} (horizontal planes x-y) and we interpolate each element $n = 1, \ldots, 44$ of the vectors $\mathbf{a}(k)$. obtaining the corresponding 3D matrices $M_{z_1}(x, y, n)$ and $M_{z_2}(x, y, n)$ of optimal parameters. Finally, we perform a linear interpolation on all the n optimal parameters in $M_{z_1}(x, y, n)$ and $M_{z_2}(x, y, n)$ along the spatial coordinate z, obtaining the 4D matrix $M(x, y, z, n)$. With $M(x, y, z, n)$, it is possible to optimize the output of the kinematic model at the i-th step and select the optimization parameters for the next iteration.

C. Event and Posture Detection

The event detection algorithm (EDA) is responsible for the estimation of the instants when lift t_l and release t_r occur [4]. Here, the EDA combines the information of hand height $\overline{p}_{Wz}(t)$, average velocity $\overline{\mathbf{v}}_{Wz}(t)$, relative velocity $\Delta\mathbf{v}_{Wy}(t)$, and the EMG signal to estimate t_l and t_r, as shown in Figure 2.

In this work, the posture detection algorithm (PDA) is a heuristic-based HAR and is responsible for continuously recognizing the posture of the user. It monitors relevant joint angles to distinguish three main activities: standing, stooping, and squatting. Such classification allows to select the appropriate map of parameters $M(x, y, z, n)$, improving the kinematic model estimations.

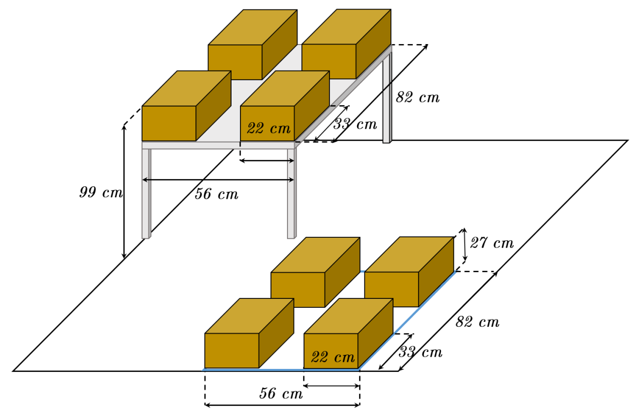

Fig. 3. Perspective view of the experimental setup reporting the measurements needed to calculate the NIOSH.

D. Experimental Setup

The ergonomic evaluation has been preliminarily evaluated with an experiment on a healthy subject (age: 37 years; height: 178 cm; weight: 75 kg), selected as part of the 50^{th} percentile of the European worker population. The experimental protocol was approved by the Ethical Committee of Liguria, Italy, 8 October 2019, protocol number: 001/2019, and complied with the Helsinki Declaration. After receiving a full explanation of the experimental procedure, the subject signed a consent form. The participant wore the TB-SS, which was used to record IMU data at 50 Hz and EMG data at 200 Hz. At the beginning of the testing session, the subject completed the suit calibration procedure to ensure initial sensor-to-body alignment.

The experimental session simulated a realistic MMH activity, which is common across industrial sectors where logistic tasks are carried out. The task involved transferring loads from a pick-up point to a workstation located three steps away three times. Here, the loads were 4 boxes of 5 kg, the pick-up area was marked on the ground, as the release area on the workstation. Each box was placed precisely on the four corners of the marked pick-up area. According to the order of execution, the boxes on the ground were identified by the terms: close left (CL) and far left (FL), close right (CR) and far right (FR). In relocating the boxes on the workstation, the subject filled the release area in reverse order, starting from the back, so that the CL box on the ground became the FL on the desk. Figure 3 details the geometry of the environment and the task. Before starting the MMH activity, the subject was asked to simulate it by placing both hands on each of the boxes while squatting and stooping, see Figure 4a and b. The subject was also asked to simulate the release phase while standing in front of the workstation, see Figure 4c. In this way, it was possible to record the data and perform the PSSC to generate the two maps of parameters M_1 and M_2, enabling a precise reconstruction of the user kinematics, see Figure 4d-f. The former corresponded to the *stand-to-squat* action, the latter to the *stand-to-stoop* action. During MMH activity, the subject

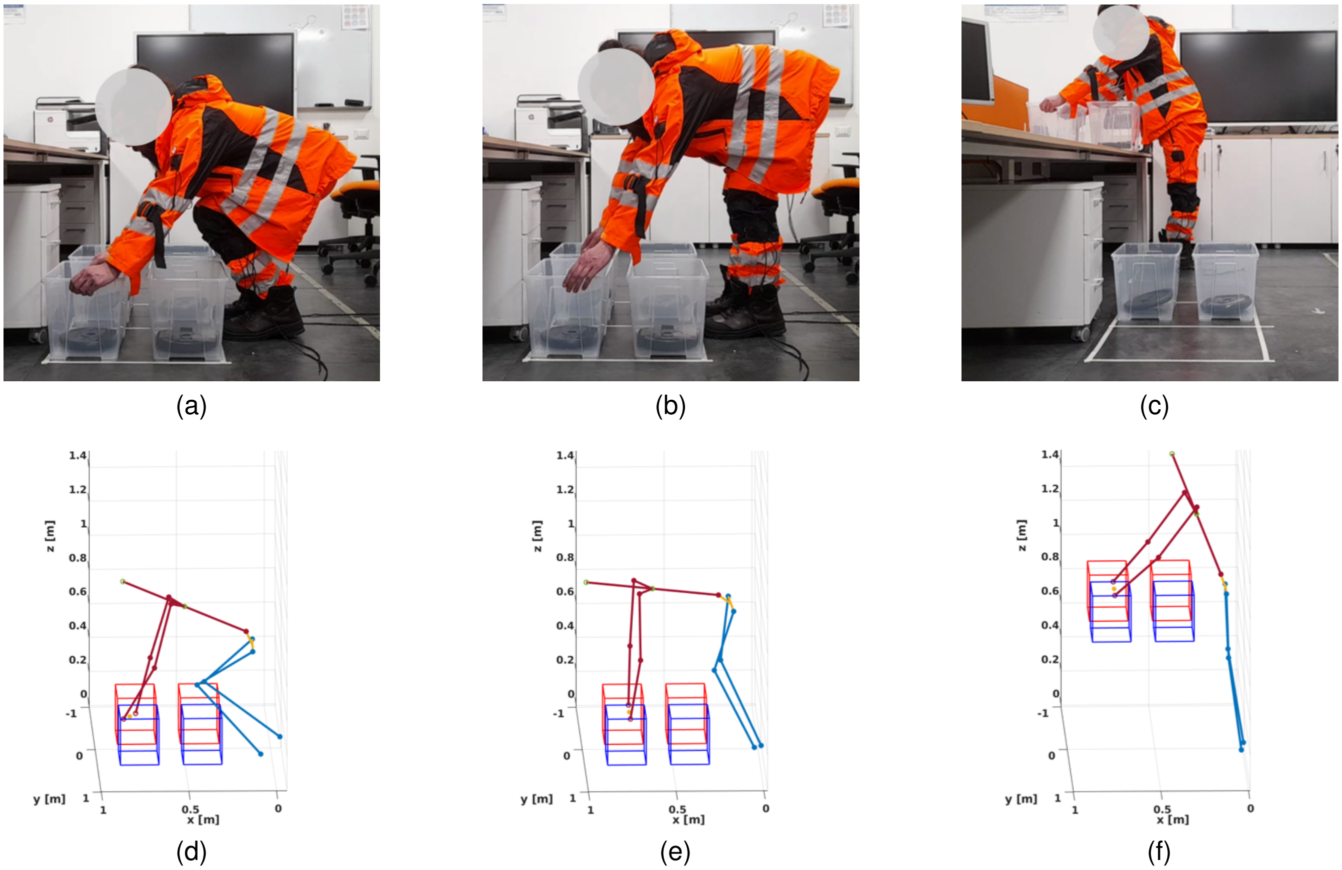

Fig. 4. The posture-specific spatial calibration (PSSC) procedure and the kinematic reconstruction. (a) The subject squats and reaches the FL box. (b) The subject stoops and reaches the box. (c) The subject stands and reaches the box. (d) Kinematic reconstruction of squat posture. (e) Kinematic reconstruction of stoop posture. (f) Kinematic reconstruction of stand posture.

was asked to stand in front of the pick-up area, execute the task at a self-selected speed, and select the preferred lifting technique, e.g., stoop or squat. Before the experimental session, the investigator carried out the ergonomic assessment based on the NIOSH lifting index by annotating the relevant parameters. A video of the experimental section was shot to support the observational evaluation process with visual feedback.

III. RESULTS

All the data from the TB-SS were processed using Matlab (R2021b version, The MathWorks Inc, USA). The proposed kinematic optimization based on the PSSC methodology has been validated preliminarily on a single subject. We manually measured all the geometrical parameters of the MMH task. Then, we evaluated the Cartesian errors $\mathbf{e}_{nO}$ and $\mathbf{e}_O$ of the non-optimized (nO) and optimized (O) kinematic models, respectively, during the pick-up (P) and release (R) phases. These errors measure the difference between the midpoint between the hands of the user $\overline{\mathbf{p}}_W(t)$ and the known positions of the boxes P_k. For each box, the EDA identified the moments $t = t_l$ and $t = t_r$ when lifting and release occur, see Figure 2. Throughout the activity, the PDA classifies the posture of the user and selects the appropriate map of parameters $M(x, y, z, n)$. Table I reports the cumulative average values and the standard deviation of the errors $\mathbf{e}_{nO}$ and $\mathbf{e}_O$ over the three repetitions. During the pick-up phases, the PSSC algorithm improves the accuracy of the kinematic model by 63.8%, 8.9%, and 44.8% along the x, y, and z axes, respectively. The error modulus improves by 41.2% thanks to the algorithm. During the release phases, the PSSC algorithm improves the model accuracy by 42.1%, 56.4%, and 77.0% along the x, y, and z axes, respectively. The error modulus improves by 59.3% thanks to the algorithm.

TABLE I

NON-OPTIMIZED (NO) AND OPTIMIZED (O) AVERAGE ESTIMATION ERRORS $\mathbf{e}_{nO}$ AND $\mathbf{e}_O$ OVER THE THREE REPETITIONS DURING THE PICK-UP (P) AND RELEASE (R) PHASES OF THE MMH ACTIVITY

	$x\ [mm]$	$y\ [mm]$	$z\ [mm]$	$\lvert \cdot \rvert\ [mm]$
$\mathbf{e}_{nO}$ (P)	155 ± 73	78 ± 40	49 ± 26	189 ± 65
$\mathbf{e}_{nO}$ (R)	95 ± 72	124 ± 66	135 ± 25	221 ± 59
$\mathbf{e}_O$ (P)	56 ± 47	71 ± 53	27 ± 20	111 ± 42
$\mathbf{e}_O$ (R)	55 ± 36	54 ± 32	31 ± 21	90 ± 39

With the observational method, we evaluated the NIOSH multipliers related to the MMH performed and the corresponding lifting index (LI). The results are reported in table II. The same parameters were calculated digitally using the

TABLE II

MANUALLY MEASURED NIOSH PARAMETERS AND THE CORRESPONDING LIFTING INDEX (LI).

Box	Hands H. (cm)	Ver. Dis. (cm)	Hor. Dis. (cm)	Twist deg	Freq.	LI kg
CL	27	72	40	31	12	0.61
CR	27	72	40	31	12	0.61
FL	27	72	74	18	12	0.92
FR	27	72	74	18	12	0.92

data from the TB-SS, the optimized kinematic model output, and the EDA. The results are reported in table III. Both tables omit the Grasp, Single Limb, and Load multiplier because these are not relevant to the scope of this work. Comparing the linear parameters in table II and III, the linear values of the non-optimized model (nO) differ significantly. Considering the absolute errors as the difference of each entry in the tables, the minimum absolute error is 3 cm, and the maximum is 20 cm. Concerning the angular parameter, the minimum absolute error of the twist is 3° and the maximum is 17°. Finally, the minimum absolute error of the lifting index is 0.12, and the maximum is 0.20. In contrast, the linear values of the optimized model (O) differ slightly from those manually measured. The minimum absolute error is 1 cm, and the maximum is 9 cm. Concerning the angular parameter, the minimum absolute error of the twist is 0° and the maximum is 9°. As a consequence, the minimum absolute error of the lifting index is 0.05, and the maximum is 0.08. Therefore, the PSSC improves the model error by 60% in calculating the task-related lifting index. The LI errors of the optimized model represent 1.6% and 2.6% of the full-scale value, respectively.

Although the very limited amount of data, the proposed PSSC method produces robust and consistent results w.r.t. time and posture of the user, especially considering that the two optimal parameter maps, M_1 and M_2, were generated before starting the MMH activity under investigation. Our optimized model surpasses the current state-of-the-art, delivering a Cartesian error of only 50 mm, representing 2.7% of whole-body kinematics. Notably, this outperforms the sensor fusion method of Johnson et al., which achieves similar error magnitudes while tracking only the user arm, representing a 10% relative error. Due to the task simplicity, the PDA is capable of identifying the user movements and selecting the corresponding map. Transitions, ambiguous and diverse postures will require a more advanced HAR algorithm [9]. Regarding the digital ergonomic evaluation, the preliminary results are comparable with those obtained in [4], where the IMU-based motion capture device was commercial and included sensors on the shoulders, hands, and feet of the users.

TABLE III

NON-OPTIMIZED (NO) AND OPTIMIZED (O) AVERAGE NIOSH PARAMETERS OVER THE THREE REPETITIONS, THE CORRESPONDING LIFTING INDEX (LI), AND THE AVERAGE ERROR W.R.T. OBSERVATIONAL VALUES.

Box	Hands H. (cm)	Ver. Dis. (cm)	Hor. Dis. (cm)	Twist deg	Freq.	LI
CL (nO)	21±2	63±4	21±8	48±20	12	0.41±0.02
(Err.)	(6)	(9)	(19)	(17)	(−)	(0.20)
CR (nO)	24±2	62±1	32±6	28±8	12	0.46±0.09
(Err.)	(3)	(10)	(8)	(3)	(−)	(0.15)
FL (nO)	22±2	60±2	54±3	25±7	12	0.78±0.05
(Err.)	(5)	(12)	(20)	(7)	(−)	(0.14)
FR (nO)	20±2	66±1	59±6	13±6	12	0.80±0.03
(Err.)	(7)	(6)	(15)	(5)	(−)	(0.12)
CL (O)	28±3	71±4	47±5	30±12	12	0.67±0.04
(Err.)	(1)	(1)	(7)	(1)	(−)	(0.06)
CR (O)	28±2	73±2	49±6	22±6	12	0.67±0.07
(Err.)	(1)	(1)	(9)	(9)	(−)	(0.06)
FL (O)	31±2	69±2	73±3	18±6	12	0.87±0.06
(Err.)	(4)	(3)	(1)	(0)	(−)	(0.05)
FR (O)	24±2	77±1	73±6	12±7	12	0.84±0.02
(Err.)	(3)	(5)	(1)	(6)	(−)	(0.08)

IV. CONCLUSIONS

In this work, an IMU-based IWS is used to track the user during an ordinary MMH activity, i.e., relocating boxes from a pick-up area to a workstation. We digitally evaluate the task-related ergonomic risk according to the NIOSH equation, whose parameters are estimated by reconstructing the whole-body kinematics of the user. The posture-specific spatial calibration method generates two maps of optimal parameters that compensate for the IMU estimation errors. Here, a heuristic-based human activity recognition algorithm allows to select the appropriate map according to the user posture and, as a result, the user kinematics is reconstructed with an average error of 50 mm. Thanks to the event detector algorithm all the phases of the MMH activity are identified correctly, allowing precise evaluations of the NIOSH parameters with limited errors. Comparing the results of the non-optimized and optimized kinematics, the PSSC improves the model error by 60% in calculating the task-related LI. With respect to the observational LI, the digital evaluation differs by 0.05, representing the 1.6% of the full-scale. To confirm these results, future works will test the PSSC method on a large pool of subjects, across multiple sessions and more complex workplace configurations. Then, the PSSC method will be integrated into the TB-SS software and tested during on-site material handling.

REFERENCES

[1] J. de Kok, P. Vroonhof, J. Snijders, G. Roullis, M. Clarke, K. Peereboom, P. van Dorst, and I. Isusi, “Work-related MSDs: Prevalence, costs and demographics in the EU (final report),” European Agency for Safety and Health at Work, Luxembourg, Report, 2019, iSSN: 1831-9343. [Online]. Available: https://osha.europa.eu/en/publications/work-related-msds-prevalence-costs-and-demographics-eu

[2] H. D. of Physical Sciences, *NIOSH, Manual of Analytical Methods*. US Department of Health and Human Services, Public Health Service, Centers, 1994.

[3] J.-A. Diego-Mas, J. Alcaide-Marzal, and R. Poveda-Bautista, "Errors using observational methods for ergonomics assessment in real practice," *Human factors*, vol. 59, no. 8, pp. 1173–1187, 2017.

[4] S. Leggieri, V. Fanti, D. G. Caldwell, and C. Di Natali, "Online ergonomic evaluation in realistic manual material handling task: proof of concept," *Bioengineering*, vol. 11, no. 1, p. 14, 2023.

[5] M. Menolotto, D. Komaris, S. Tedesco, B. O'Flynn, and M. Walsh, "Motion capture technology in industrial applications: A systematic review," *Sensors*, vol. 20, no. 19, p. 5687, 2020.

[6] A. Sochopoulos, T. Poliero, J. Ahmad, D. G. Caldwell, and C. Di Natali, "Human activity recognition algorithms for manual material handling activities," *Scientific Reports*, vol. 15, no. 1, p. 10954, 2025.

[7] S. Leggieri, P. Sencandan, V. Fanti, J. Ahmad, D. G. Caldwell, and C. Di Natali, "The smart suit: a novel tool platform for learning and assessment at work," *Automation, Robotics & Communications for Industry 4.0/5.0*, p. 257, 2025.

[8] S. Leggieri, Y. Tefera, D. Caldwell, and C. Di Natali, "Kinematic optimization and spatial mapping method for efficient pose estimation in safe human-robot collaboration with imu-based mocap," *IEEE Transactions on Robotics*, (submitted).

[9] J. Ahmad, S. Leggieri, D. Caldwell, and C. Di Natali, "Real-time human activity recognition on edge devices for industrial applications," *IEEE Sensors Journal*, 2026.